

Single-scan longitudinal relaxation measurements in high-resolution NMR spectroscopy

Nikolaus M. Loening,^{a,*} Michael J. Thrippleton,^b James Keeler,^b and Robert G. Griffin^a

^a Francis Bitter Magnet Laboratory and Department of Chemistry, Massachusetts Institute of Technology, Cambridge, MA 02139, USA

^b Department of Chemistry, University of Cambridge, Lensfield Road, Cambridge CB2 1EW, UK

Received 22 March 2003; revised 19 May 2003

Abstract

Several single-scan experiments for the measurement of the longitudinal relaxation time (T_1) are proposed. These experiments result in fast and accurate determinations of the relaxation rate, are relatively robust to pulse imperfections, and preserve information about the chemical shift. The method used in these experiments is to first encode the T_1 values as a spatial variation of the magnetization and then to read out this variation either by applying a weak gradient during acquisition or by sequentially observing different slices of the sample. As a result, it is possible to reduce the time necessary to determine the T_1 values by one or two orders of magnitude. This time saving comes at the expense of the signal-to-noise level of the resulting spectrum and some chemical shift resolution.

© 2003 Elsevier Science (USA). All rights reserved.

Keywords: Longitudinal relaxation; T_1 ; Single-scan; One-shot

1. Introduction

In NMR, knowledge of the longitudinal relaxation times (T_1) for a sample is important because, in many cases, the rate at which an experiment can be repeated is limited by the rate of longitudinal relaxation. Typically, a delay 3–5 times that of the longest longitudinal relaxation time is inserted in between every scan of the NMR experiment. This is to avoid saturating the nuclear spins and also ensures that residual transverse magnetization from previous scans does not interfere with the current scan.

Longitudinal relaxation times are usually measured using the inversion recovery (IR) experiment (Fig. 1a). In this experiment, the sample magnetization is inverted by a π -pulse and then, after a delay Δ , rendered transverse and observed. The intensity S of a peak in the spectrum depends on Δ and T_1 according to

$$\frac{S}{S_0} = 1 - 2 \exp\left(-\frac{\Delta}{T_1}\right), \quad (1)$$

where S_0 is the the signal intensity as $\Delta \rightarrow \infty$. By repeating the IR experiment with a number of different values for Δ , it is possible to extract the value of T_1 by fitting the data to Eq. (1). The IR experiment works quite well for measuring longitudinal relaxation times, but suffers the disadvantage of being relatively slow. This is because a series of experiments with different values of Δ must be acquired and, in order to measure T_1 values accurately, the delay between scans must be five or more times longer than the longest T_1 in the sample. Consequently, a large amount of experiment time may be required to sample the full range of the IR curves.

An alternative method that is often used to more quickly determine T_1 values is to search for the “null point” of the IR curve. The null point is the time at which the signal intensity goes through zero and is given by

$$\Delta = T_1 \ln(2). \quad (2)$$

By searching for the null point, it is usually possible to get a quick estimate of the longest T_1 value for the system in only a few experiments. However, this method requires the active intervention of the user, does not

* Corresponding author. Fax: 1-617-253-5405.

E-mail address: Niko_Loening@alumni.hmc.edu (N.M. Loening).

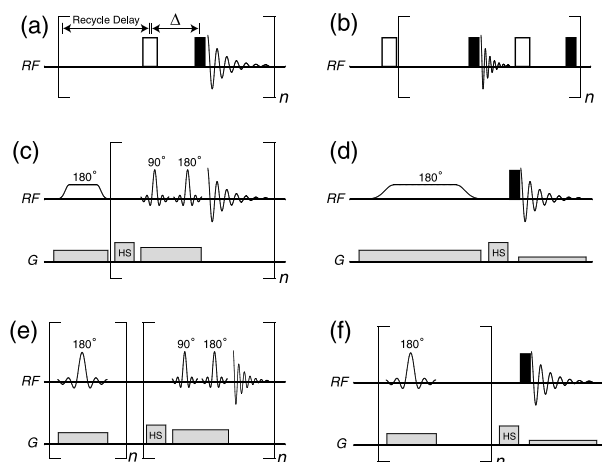


Fig. 1. T_1 measurement experiments. The experiments shown are: (a) the IR sequence; (b) the triplet pulse sequence; (c) the continuous MA-IR sequence; (d) the continuous PI-IR sequence; (e) the discrete MA-IR sequence; and (f) the discrete PI-IR sequence. Hard pulses are indicated by rectangles (filled for $\pi/2$ -pulses, hollow for π -pulses), slice-selective pulses are indicated by sinc functions, and adiabatic inversion pulses are indicated by “wurst” shapes. The bracketed blocks indicate the part of the pulse sequence that is repeated n times to record the inversion recovery curve. Read gradients are indicated by low power gradient pulses and homospoil gradient pulses are indicated by “HS”; all other gradients are for slice-selection.

result in precise measurements of T_1 , and still requires several scans.

In this paper, we present several experiments that allow the accurate determination of longitudinal relaxation times in a single experiment (i.e., a single scan). Pulse sequence diagrams of these experiments are shown in Figs. 1c–f. The approach that we use is similar to one that we have recently presented for the measurement of diffusion coefficients [1,2]. Namely, the parameter of interest is encoded as a spatial variation in the sample magnetization and then read out using imaging techniques. However, unlike previous single-scan sequences for measuring T_1 values, our experiments preserve chemical shift information and are therefore applicable to samples with multiple resonances. In addition, the results do not depend on the transverse relaxation time (T_2) and the experiments are relatively robust with respect to pulse miscalibration. Acquiring all the T_1 values of a sample in a single-scan does incur some trade-offs. In comparison to the standard IR pulse sequence, these trade-offs are a decrease in sensitivity and, in some cases, a reduction in chemical shift resolution.

It is only fair to mention that some of the T_1 measurement experiments that we present here are in certain ways very similar to experiments reported previously [3,4]. However, whereas the previous experiments were designed for magnetic resonance imaging, the experiments presented here are suitable for high-resolution NMR spectroscopy: the experiments presented in this paper are designed to preserve information about the chemical shift rather than spatial information.

2. Theory

Single-scan experiments for measuring T_1 are not a new idea; many examples exist in the literature [5–9] and variations of these techniques are not uncommon in MRI. The drawback to almost all these experiments is that they lack chemical shift resolution and/or return a value that reflects a combination of longitudinal and transverse relaxation.

Perhaps the oldest example of a single-scan T_1 measurement sequence is the triplet pulse sequence [5] shown in Fig. 1b and its later variations [6,7]. In the triplet pulse sequence, the sample magnetization is first inverted. Then, as the magnetization relaxes back to its equilibrium value, it is rendered transverse, observed, refocused by a spin-echo, and then restored to the longitudinal axis. This “triplet” of radiofrequency (RF) pulses is repeated a number of times while the spins are relaxing back to equilibrium so that the full IR curve is sampled.

The main problem with this approach is that it is not useful for spectra that contain multiple resonances. This is because, to resolve multiple resonances, the observation time (i.e., the spin-echo period) must be lengthened. As the spin-echo period becomes longer, the measured data cannot be assumed to reflect only longitudinal relaxation. Rather, the data reflect a combination of longitudinal and transverse relaxation. In addition, the spin-echo period makes the analysis of systems with homonuclear couplings problematic due to the generation of antiphase magnetization during each spin-echo. Finally, errors due to pulse imperfections can accumulate over the course of such an experiment.

To get around the limitations of previous single-scan T_1 measurement experiments, we have developed several new pulse sequences. The general method that we employ in these experiments is to prepare the magnetization differently in different parts of the sample. The data is then acquired in such a way that the spatial-modulation of the magnetization is reflected in the spectrum. As will be seen later in this paper, this method allows the retention of chemical shift information and is less affected by homonuclear couplings than previous single-scan methods. However, the greater applicability of the technique comes at the expense of sensitivity. This reduction in sensitivity arises because only a portion of the sample volume is observed or because the signal is broadened during acquisition by a small gradient. Nevertheless, the methods that we present here are likely to be useful in situations where the sensitivity is high, as is often the case in ^1H NMR of small molecules.

The single-scan methods described in this paper can be considered as a subset of a “new” method for acquiring multidimensional data in NMR spectroscopy. In a conventional multidimensional NMR experiment, the signal variation in the indirect dimensions is determined by incrementing one or more delay times. However, the

signal variation can be also encoded as a variation along a spatial axis of the sample (as described in [1,2]). If a number of scans are collected using a series of orthogonal spatially selective pulses, it is theoretically possible to use a Hadamard transform [10] followed by the usual multidimensional Fourier transform to generate a spectrum with the same signal-to-noise level as that which is achieved using the conventional acquisition method. As both methods offer the same sensitivity per unit time, there is no compelling reason to switch from the conventional acquisition method for multiple scan experiments. However, in the case of single-scan experiments, our method has several advantages. We note that, recently, a similar technique has been independently developed for the acquisition of homonuclear correlation experiments [11].

2.1. Spatial modulation of the magnetization

The first step in all of our single-scan T_1 measurement experiments is to encode the T_1 values of the sample as a spatial variation of the sample magnetization. This can be accomplished by either of two methods, which we refer to as discrete and continuous encoding.

In discrete encoding, a series of slice-selective pulses are used to invert different parts of the sample at different times. The result is a magnetization profile where the magnetization will have a constant value within a given slice of the sample, but will vary from slice to slice. Slice-selection is accomplished by applying a shaped RF pulse in conjunction with a magnetic-field gradient pulse; this results in the inversion of the magnetization for a slice of the sample while not affecting magnetization outside of that slice (at least in the ideal case). This methodology was used for the pulse sequences shown in Figs. 1e and f.

In the continuous encoding method, as shown in Figs. 1c and d, the magnetization varies smoothly as a function of distance along the axis of the magnetic-field gradient. Such a variation can be achieved by applying a frequency-swept adiabatic inversion pulse in synchronicity with a magnetic-field gradient pulse. This works because the gradient makes the offset frequencies of the resonances vary according to position and the adiabatic pulse inverts different offsets at different times during the pulse.

Although experiments employing continuous encoding are more elegant, in actual practice, discretely encoded experiments prove to be more practical because the variation in the magnetization can be made to match the way that the magnetization is sampled. In addition, for the experiments discussed here, the discrete experiments make less stringent demands on the NMR hardware.

2.2. Reading the magnetization profile

Once the magnetization has been spatially encoded, the encoding needs to be “read-out” in a single scan

while retaining information about the chemical shift. In our experiments, this is done in two ways: multiple acquisition (MA) and parameter imaging (PI).

In MA experiments, the time-domain data corresponding to different regions of the sample are measured sequentially. This is accomplished by using a series of slice-selective excitation pulses, each of which is followed by an acquisition period. The result is a two-dimensional data set in which the spatial encoding is reflected in the indirect dimension. Unlike the triplet pulse sequence discussed previously, the MA approach is not sensitive to pulse imperfections, homonuclear couplings, or transverse relaxation, as no attempt is made to refocus the magnetization and “reuse” it. The pulse sequences shown in Figs. 1c and e are examples of MA T_1 measurement experiments. Note that, in our experiments, a slice-selective spin-echo is used to excite the magnetization instead of a single slice-selective excitation pulse. This ensures that phase errors from the slice-selective $\pi/2$ -pulse are refocused. In addition, a homospoil gradient pulse is included before every acquisition loop to ensure that magnetization from one acquisition does not interfere with the next.

In PI experiments, the signal is acquired in the presence of a weak magnetic-field gradient. The gradient broadens each line in the spectrum to a certain extent so that, after Fourier transformation of the time-domain data, each peak in the spectrum becomes a small image of the sample. These sample images reflect the spatial encoding of the magnetization and can be analyzed to determine the relevant parameter. This methodology was incorporated in the pulse sequences shown in Figs. 1d and f, and in the experiments that we have reported previously for the measurement of diffusion coefficients in a single-scan [1,2].

In general, both of these approaches are applicable for the measurement of most spectroscopic parameters; each has its advantages and disadvantages. For the case of T_1 measurements, both MA and PI experiments can be used. As will be seen later in this paper, MA experiments are usually preferable for T_1 measurements as they have better chemical shift resolution and tend to be easier to analyze than PI experiments. These advantages arise because the parameter of interest is determined in a separate dimension rather than projected into the directly detected dimension.

3. Experimental

All experiments were conducted on a Bruker DRX600 spectrometer equipped with a 5 mm inverse geometry, z -axis gradient probe. The sample consisted of adenosine 5'-monophosphate (AMP), *N*-acetylvaline (NAV), and *N*-acetylglycine (NAG) dissolved in deuterated water.

The concentrations of AMP, NAV, and NAG, were 27, 63, and 85 mM, respectively.

A magnetic field gradient of 46 G cm^{-1} was used for the homospoil pulses in all the experiments.

For the MA experiments, gaussian pulses with a 1% truncation level were used for slice-selective excitation and refocusing. Different slices were excited by stepping the frequency offset for the selective pulses from 24 to -32 kHz in 8 kHz steps; these pulses were applied synchronously with a 11 G cm^{-1} magnetic field gradient. The slice-selective $\pi/2$ -pulses used a RF field strength of 1 kHz ; for the slice-selective π -pulses the RF field strength was 2 kHz . Inversion of the magnetization was accomplished using a hyperbolic secant to ensure uniform inversion across the sample. Eight acquisition periods were used to sample the IR curves. Each acquisition cycle was approximately 0.51 s long, so the total experiment time was 4 s .

For the PI experiments, a gradient of 0.012 G cm^{-1} was used during acquisition to “read-out” the T_1 values. For the discrete variant of the experiment, hyperbolic secant pulses were used to selectively invert different regions of the sample. The frequency offsets of these pulses varied between 96 and -128 kHz in steps of 32 kHz . These pulses were applied in conjunction with a 55 G cm^{-1} gradient. A delay of 0.5 s was used between each inversion pulse, resulting in an experiment time of 4 s .

In the continuous PI–IR experiment, a WURST pulse [12] was used as the frequency-swept adiabatic inversion pulse. The length of this pulse was 3 s , and a RF field strength of 500 Hz was used. A 0.056 G cm^{-1} magnetic field gradient was applied during the inversion pulse to make the time of inversion spatially dependent. The total time for the continuous PI–IR experiment was 3.5 s .

For comparison, T_1 values for the sample were determined using a conventional IR experiment (Fig. 1a). The recycle delay was set to 40 s to ensure that accurate T_1 values could be measured for all resonances including the slowly relaxing water signal. An eight step phase cycle was used for each of eight increments; the total experiment time was 43 min .

For comparisons of the total experiment time, it is more appropriate to compare the single-scan experiments with a variant of the conventional IR experiment which uses a homospoil after the inversion pulse and does not include phase cycling. Such an experiment would have required 5 min to complete.

4. Results

4.1. Continuous experiments

By using a frequency-swept adiabatic inversion pulse in conjunction with a pulsed field gradient, it is possible

to construct continuous versions of the single-scan T_1 measurement sequences. One example is the continuous PI–IR experiment (Fig. 1d), which was used to produce the spectrum shown in Fig. 2. Unlike the discrete PI–IR experiment discussed later, the continuous experiment results in a smoothly varying lineshape. As a result, it is possible for many more points to define the IR curve than in the discrete experiments.

Although the continuous experiments are somewhat simpler experimentally than the discrete versions, the reality is that the continuous experiments are not as useful due to the limitations of the spectrometer hardware. The problem is that the time at which the magnetization is inverted depends on its offset, and the offset depends on the chemical shift as well as the position of the magnetization along the gradient axis. In discrete experiments, it is possible to use large values for the gradient as the inversion pulses are relatively short (on the order of 1 ms or less). Therefore, the dominant contribution to the offset in discrete experiments is the spatial position of the spin.

In the case of the continuous experiments this is not the case as the gradient and the adiabatic pulses must be applied for a period that is 3 – 5 times the length of T_1 . This time period is usually on the order of one or more seconds, a length of time which severely constrains the maximum strength of these pulses. Consequently, the encoding depends in part on the chemical shift. This effect is clearly seen in Fig. 2 if one compares the upfield resonance to the downfield resonance: the position of the IR curve is shifted to one side or the other within the lineshape. Although this shift can be accounted for in the data analysis, it still poses a problem because in most cases the range of chemical shifts is large enough that it

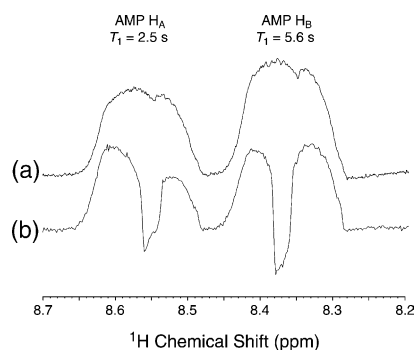


Fig. 2. A portion of the continuous PI–IR spectrum of the AMP, NAV, and NAG mixture showing: (a) the spectrum in the presence of a weak read gradient and (b) the continuous PI–IR spectrum. The left and right peaks, labeled H_A and H_B , correspond to the adenine ring protons of AMP. These protons have T_1 values of 2.5 and 5.6 s , for H_A and H_B , respectively. The position of the inversion curve within the lineshape strongly depends on the chemical shift offset. This is a consequence of instrumental limitations. Note that some of what appears to be noise in the spectrum is actually due to instrumental artifacts that are accounted for in the data analysis.

is not possible to cover all of the resonances with the adiabatic sweep. Although somewhat less conservative values than those used in this study can be used for the RF field and gradient strengths, the interplay between chemical shift and spatial encoding will remain significant in continuous IR experiments unless unusually robust gradient and/or RF coils are used. As a result of this complication, we will only consider the discrete versions of both the PI-IR and the MA-IR experiments in the following discussion.

4.2. The discrete MA-IR experiment

The result of using the discrete MA-IR experiment (Fig. 1e) with the AMP, NAV, and NAG sample is shown in Fig. 3. The figure shows a stacked plot of the data after Fourier transformation in the direct dimension. The form of the IR curve is clearly visible in the indirect dimension. Visually, it can be seen that the NAV H_γ resonances at 0.9 ppm relax more quickly than the AMP and NAG H_α resonances between 4.0 and 4.5 ppm. The narrow resonances at 2.0 ppm are from the methyl protons of the NAV and NAG acetyl groups. The T_1 values of these two resonances differ, resulting in the apparent “antiphase” lineshape in the fourth row of the spectrum. Note that these resonances are only 3.5 Hz apart from one another; this demonstrates the high chemical shift resolution possible in a single-scan using the MA-IR technique.

The discrete MA-IR experiment that we used is not exactly the same as the experiment shown in Fig. 1e. It turns out that in the case of T_1 measurements, it is possible to invert the sample using a single non-selective inversion pulse instead of performing a series of slice-selective inversions. This can be done because the on-going process of longitudinal relaxation during the experiment provide the necessary spatial variation. The use of a series of slice-selective inversion pulses has a small advantage over using a single non-selective

inversion pulse in that it is possible to tune the sequence to a certain extent in order to optimize the balance between the length of each acquisition and the spacing of the points on the IR curve. However, this advantage is offset by the added complication of implementing a series of slice-selective inversion pulses and, therefore, we have opted to use only a single non-selective inversion pulse in our experiments; the resulting pulse sequence is shown in Fig. 4.

The peak intensities for all the resonances decrease for longer IR delays; this is a result of two effects. The primary cause is the variation in the homogeneity of the main magnetic field across the sample; the shimming is better for portions of the sample that are in the center of the RF coil than for portions that are near the edges. Consequently, the linewidths vary from increment to increment, resulting in the observed decrease in signal intensity for increments corresponding to sample at the edges of the RF coil. However, this does not actually affect the results as the integrals of the peaks, rather than their intensities, are used for estimating the T_1 values. The second cause for the observed variation in signal intensity is the inhomogeneity of the RF coil. This effect is accounted for in the data analysis, as described later.

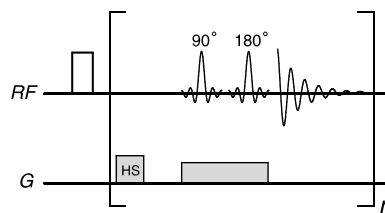


Fig. 4. The pulse sequence used for the discrete MA-IR experiment. A single non-selective pulse is used instead of the series of slice-selective pulses depicted in Fig. 1e because longitudinal relaxation during the course of the experiment provides the necessary spatial variation of the magnetization.

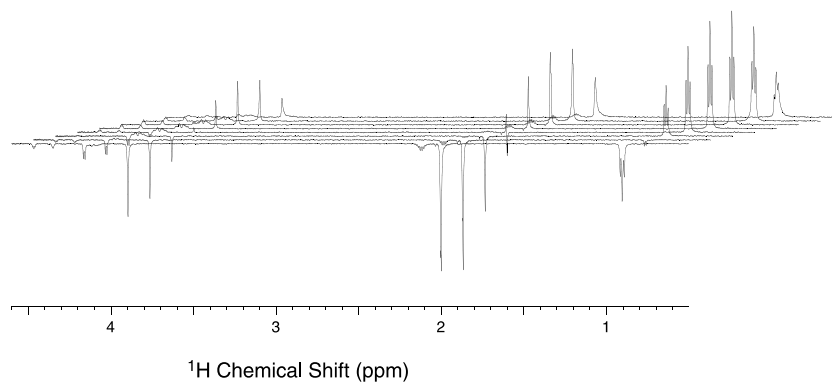


Fig. 3. A portion of the IR spectrum resulting from a single-scan T_1 measurement using the discrete MA-IR experiment shown in Fig. 4. The sample consisted of a mixture of AMP, NAV, and NAG in deuterated water, as described in the text. Eight slice-selective acquisitions were used, resulting in a total experiment time of 4 s.

4.3. The discrete PI–IR experiment

In the discrete PI experiment (Fig. 1f), the IR curve is discretely encoded into the lineshapes of the spectral resonances by a series of slice-selective inversion pulses. Consequently, the T_1 values can be extracted by fitting the profiles; Fig. 5 illustrates the result of such an experiment.

Fig. 6 shows a small region of the spectrum shown in Fig. 5, illustrating the variation in the lineshape due to the different T_1 values for the H_A and H_B resonances of AMP. From inspection, it is obvious that the downfield peak relaxes more rapidly than the upfield peak. One point to note is that, although the sample images look rather noisy, much of this is due to instrumental artifacts and is accounted for in the data analysis.

The primary drawback of the PI experiments, at least in comparison to the MA experiments, is the greater trade-off between information about the T_1 values and chemical shift resolution. It is clear from Fig. 5 that in order to broaden the lines such that the T_1 values are measurable, the chemical shift resolution must be curtailed. Another caveat to PI experiments is that the instrumental lineshape, the natural linewidth of the resonances, and scalar couplings will affect the results. Typically, the magnitude of the read gradient is set so that the gradient-induced broadening dominates both of the other effects. This means that these effects can be neglected in the data analysis, but this simplification comes at the expense of decreasing the chemical shift resolution. Better chemical shift resolution can be achieved by using a weaker read gradient and then using either deconvolution or a more sophisticated fitting algorithm to estimate the T_1 values. However, this greatly increases the complexity of the data analysis.

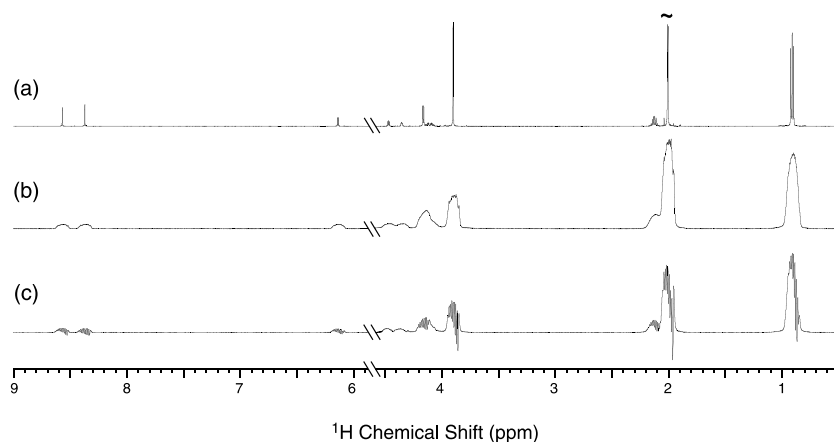


Fig. 5. From top to bottom: (a) the regular ^1H spectrum; (b) the spectrum in the presence of a weak read gradient; and (c) the discrete PI–IR spectrum for the AMP, NAV, and NAG mixture. Relative to MA experiments, PI experiments have a much larger trade-off between information about the rate of longitudinal relaxation and chemical shift resolution.

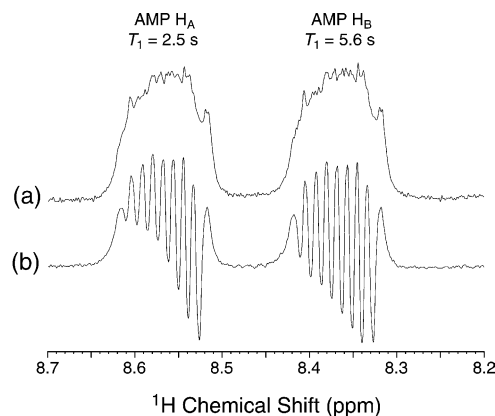


Fig. 6. A portion of the spectra shown in Fig. 5: (a) the spectrum in the presence of a weak read gradient and (b) the discrete PI–IR spectrum. The left and right peaks correspond to the H_A and H_B resonances of AMP, which have T_1 values of 2.5 and 5.6 s, respectively. Note that much of what appears to be noise in the spectrum is actually due to instrumental artifacts that are accounted for in the data analysis.

4.4. Data analysis

Although the results of the single-scan T_1 measurement experiments are not susceptible to effects from transverse relaxation, consideration does need to be taken of the homogeneity of the RF coil, the homogeneity of the gradient coil, and the effects of molecular diffusion.

Inhomogeneity of the RF coil affects the results in two ways. First, the nutation angle of RF pulses will vary between different regions of the sample. Second, the coupling of the magnetization to the coil will vary in the same manner. For all our experiments, we made the assumption that variations in the signal intensity due to variations in the nutation angle were negligible. This is valid because the signal strength depends on the nutation angle θ according to $\sin(\theta)$, and $\sin(\theta) \approx 1$ for

values of θ near to $\pi/2$. Therefore, only the variation in the coil coupling was considered. This effect was corrected for by dividing the lineshapes (for the PI experiments) or the points on the IR curve (for the MA experiments) by a reference image of the sample.

Inhomogeneities in the gradient strength result in distortions in the sample images in PI experiments and affect the size of the sample volume excited by the slice-selective pulses. As it turns out, the reference image used to correct for variations in the coil coupling suffers from the same distortions. Therefore, when the data is divided by this reference the systematic errors due to gradient inhomogeneities cancel.

The effect due to molecular diffusion is more subtle, but also more difficult to correct. Fig. 7 demonstrates the effect molecular diffusion has on the result of a discrete PI-IR experiment on a sample of H₂O in D₂O. Due to the relatively long relaxation time of the HOD resonance, the eight inversion pulses were spaced over a 14 s time period. Over this time period, molecular diffusion is not negligible and results in broadening of the features in the spectrum as the spins move from one region of the sample to another. This is especially apparent for the first slices of the magnetization to be inverted (the downfield side of the lineshape).

Diffusion cannot be easily accounted for in the data analysis because the rate of diffusion will vary not only between samples, but also between species in the same sample. Therefore, there is no easy way to “map” the effects of diffusion and correct for them, as one can do for inhomogeneities of the RF and gradient coils. Fortunately, diffusion only affects those few samples which have very long T_1 values; for most samples (including our sample of AMP, NAV, and NAG), the effect will be

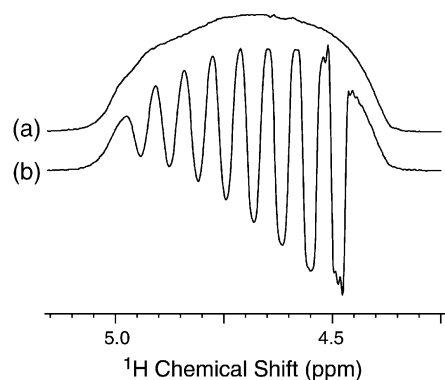


Fig. 7. Spectra of HOD in D₂O, demonstrating the impact of diffusion on discrete PI spectra. The top spectrum shows the sample image (a) whereas the bottom spectrum shows the discrete PI-IR spectrum (b). In the lower spectrum, it is apparent that components of the sample that have been recently inverted (corresponding to features on the right of the spectrum) are more sharply defined than those that have been inverted earlier in the experiment (the features on the left). This effect comes as a result of molecular diffusion during the course of the experiment.

much smaller and can be considered negligible for all but the solvent resonances. This is for two reasons: larger molecules have slower rates of molecular diffusion and larger molecules tend to relax more quickly, so the experiment can be conducted on a shorter timescale.

Molecular diffusion can also affect conventional IR T_1 measurement experiments because sample that was outside of the coil during the inversion pulse can diffuse into the active region of the NMR coil. However, this effect is small, so both conventional IR experiments and the MA-IR experiment shown in Fig. 4 are much less susceptible to diffusion than PI-IR experiments.

4.5. Comparison of the techniques

The estimated T_1 values for the various resonances in sample spectra using discrete MA, discrete PI, and conventional IR experiments are shown in Fig. 8. The results from the discrete MA-IR experiment closely match the results from the conventional experiment; none of the results differ by more than 10% between the two experiments.

The outcome of the discrete PI-IR experiment is less accurate, largely due to the effects that scalar couplings, the instrumental lineshape, molecular diffusion and the natural linewidth have on the results. Due to decreased spectral resolution in the PI-IR experiment, the T_1 values could not be estimated for three of the peaks in the spectrum.

5. Conclusion

In this paper, we have demonstrated single-scan experiments that can be used to determine the rate of longitudinal relaxation. These experiments offer a reduction in experiment time of one to two orders of magnitude in comparison to the conventional inversion recovery experiment. However, the reduction in

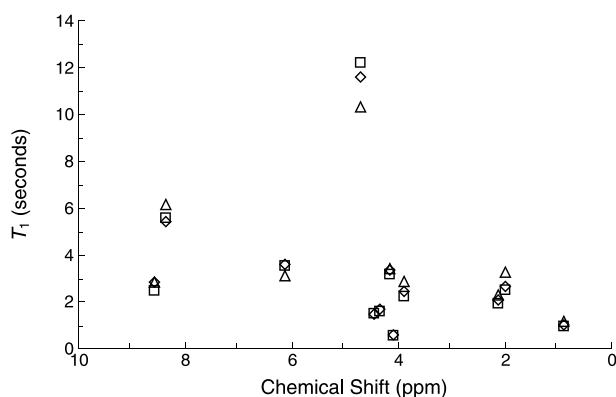


Fig. 8. The estimated T_1 values for the various peaks in the spectrum measured using the discrete MA (diamonds), discrete PI (triangles), and conventional IR (squares) sequences.

experiment time comes at the expense of sensitivity and some chemical shift resolution. Nevertheless, these methods are superior to previously described single-scan techniques.

Of the single-scan experiments presented in this paper, we believe that the discrete MA–IR experiment is the best suited for estimating T_1 values in a single-scan: this experiment has the best chemical shift resolution, yields the most accurate T_1 values, and results in spectra that are relatively easy to analyze.

The two methods used for measuring the rate of longitudinal relaxation in this paper can also be used for the measurement of other spectroscopic parameters. We have already demonstrated the use of PI techniques for measuring diffusion coefficients [1,2] and in the future we plan to show how these methods can be used in other single-scan experiments for correlation spectroscopy and for detecting sample convection.

Acknowledgments

N.M.L. thanks the National Institutes of Health (USA) for support via a National Research Service Award post-doctoral fellowship (F32 NS42425-01). N.M.L. and R.G.G. acknowledge support from the National Institutes of Health (GM-38352 and RR-00995). M.J.T. and J.K. thank the EPSRC (UK), The Newton Trust (Cambridge, UK), and Procter & Gamble for their support.

References

- [1] N.M. Loening, J. Keeler, G.A. Morris, One-dimensional DOSY, *J. Magn. Reson.* 153 (2001) 103–112.
- [2] M.J. Thrippleton, N.M. Loening, J. Keeler, A fast method for the measurement of diffusion coefficients: one-dimensional DOSY, *Magn. Reson. Chem.* 41 (2003) 441–447.
- [3] E. McVeigh, A. Yang, E. Zerhouni, Rapid measurement of T_1 with spatially selective pre-inversion pulses, *Med. Phys.* 17 (1990) 131–134.
- [4] J.G. Pipe, A fast method for obtaining a “continuous” sample of the inversion-recovery curve using spatially swept adiabatic inversion, *J. Magn. Reson.* 99 (1992) 582–589.
- [5] R.L. Streever, H.Y. Carr, Nuclear magnetic resonance of Xe^{129} in natural Xenon, *Phys. Rev.* 121 (1961) 20–25.
- [6] R.J. Kurland, R.G. Parrish, The half-wave triplet pulse sequence for determination of longitudinal relaxation rates of single line spectra, *J. Magn. Reson.* 17 (1975) 295–300.
- [7] H.T. Edzes, An analysis of the use of pulse multiplets in the single scan determination of spin–lattice relaxation rates, *J. Magn. Reson.* 17 (1975) 301–313.
- [8] J. Kronenbitter, A. Schwenk, A new technique for measuring the relaxation times T_1 and T_2 and the equilibrium magnetization M_0 of slowly relaxing systems with weak NMR signals, *J. Magn. Reson.* 25 (1977) 147–165.
- [9] J.R. Moore, K.R. Metz, Single-scan simultaneous measurement of NMR spin–lattice and spin–spin relaxation times, *J. Magn. Reson. A* 101 (1993) 84–91.
- [10] R. Freeman, *Spin Choreography: Basic Steps in High Resolution NMR*, Oxford University Press, Oxford, UK, 1998.
- [11] L. Frydman, T. Scherf, A. Lupulescu, The acquisition of multidimensional NMR spectra within a single scan, *Proc. Natl. Acad. Sci. USA* 99 (2002) 15858–15862.
- [12] Ě. Kupče, R. Freeman, Adiabatic pulses for wideband inversion and broadband decoupling, *J. Magn. Reson. A* 115 (1995) 273–276.